



CHORUS

This is the accepted manuscript made available via CHORUS. The article has been published as:

Nonequilibrium Composition Profiles of Alloy Quantum Dots and their Correlation with the Growth Mode

X. B. Niu, G. B. Stringfellow, and Feng Liu

Phys. Rev. Lett. **107**, 076101 — Published 9 August 2011

DOI: [10.1103/PhysRevLett.107.076101](https://doi.org/10.1103/PhysRevLett.107.076101)

Non-equilibrium Composition Profiles of Alloy Quantum Dots and their Correlation with Growth Mode

X. B. Niu¹, G. B. Stringfellow^{1,2}, Feng Liu^{1,*}

¹*Department of Materials Science and Engineering University of Utah, Salt Lake City, UT 84112*

²*Department of Electrical and Computer Engineering, University of Utah, Salt Lake City, Utah 84112*

Equilibrium composition profiles (CPs) of epitaxial alloy quantum dots (QDs) are well established theoretically. However non-equilibrium CPs may occur experimentally. Using an atomistic-strain-model Monte Carlo simulation method, we demonstrate a striking correlation between the non-equilibrium CP of QD and the kinetic growth mode: the layer-by-layer growth (LG) and faceted growth (FG) form a core-shell structure having the triangle core of the unstrained and V-shaped core of the strained component, respectively, and both are distinctively different from the equilibrium CP. Comparing simulations with experiments, we infer that the InGaAs dots on GaAs grow by the FG, while GeSi dots on Si grow first by the LG followed by the FG. Our findings suggest a possible method for controlling the CPs of QDs by selecting the growth mode.

PACS numbers: 68.35.Dv, 68.65.Hb, 81.07.Ta

Heteroepitaxial growth of strained thin films provides one of the most promising methods for producing quantum dots (QDs) [1]. A variety of device functions may be realized by the formation of alloy QDs with desirable composition profiles (CPs) to form inner heterostructures within the dots. Spontaneous alloy decomposition, coupled with QD morphological evolution, occurs naturally as a means of strain relaxation. Experiments demonstrate the formation of complex QD CPs, with different core shapes and accumulation of either the strained [2, 3] or the unstrained [2, 4] component in the core of QDs. A fundamental reason for the observed complex alloy CPs in QDs is that epitaxial growth is inherently a non-equilibrium process. Consequently, the resulting alloy CP in QDs is often kinetically limited, depending on growth conditions. However, our current knowledge of understanding is based mostly on equilibrium theories [5, 6], which establish the equilibrium CP governed by thermodynamics of alloy mixing in relation to strain and QD morphology. Therefore, it is highly desirable to study the non-equilibrium CPs of alloy QDs governed by growth kinetics.

One important kinetics process is diffusion. If the diffusion were unlimited, the equilibrium CP would, of course, be achieved throughout the QD. In reality, however, bulk diffusion is negligible at typical growth temperatures. On the other hand, local equilibrium alloy CP can be established during growth [7] in the near surface region due to the more rapid surface (and sub-surface) diffusion. Consequently, the kinetic growth mode, which dictates the manner of surface mass transport and alloy mixing in the growth front (i.e., surface and sub-surface regions), becomes a key factor in determining the kinetically limited overall non-equilibrium QD CP.

In this Letter, we report a theoretical study of non-equilibrium CPs of strained alloy semiconductor QDs under several different kinetic growth conditions, using an atomistic-strain-model Monte Carlo (MC) simulation

method [8]. Our simulations reveal a striking correlation between the non-equilibrium CPs of QDs and the kinetic growth mode. The growth-mode-controlled alloy CPs are distinctly different from the equilibrium CPs. By comparing the simulated CPs with experiments, we infer the kinetic modes involved in the growth of InGaAs QDs on GaAs versus GeSi QDs on Si.

For a qualitative study of the general mechanisms of spontaneous alloy phase separation, we used a two-dimensional (2D) atomistic strain model on a square lattice to calculate the Gibbs free energy of coherently strained alloy QDs on a substrate, as shown in Fig. 1. System size was tested up to a few tens of thousands of lattice points. This simple, generic 2D model should capture the essential physics during the formation of composition gradients in strained alloy structures. As a support, we have done a few testing 3D simulations which show the qualitatively same results [9]. Without losing generality, we have chosen atomic strain potential parameters corresponding to GeSi alloys as a model system. In the following, results of $\text{Ge}_{0.3}\text{Si}_{0.7}$ QDs are shown as examples and similar results are obtained with other Ge

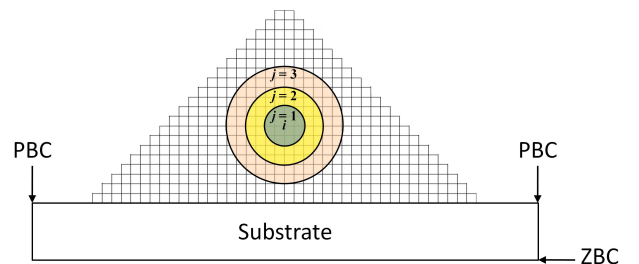


FIG. 1: (Color online) Schematic illustration of simulation framework of a 2D square lattice. Periodic boundary conditions (PBC) in the lateral direction and zero boundary condition (ZBC) at the bottom of the substrate are used. Circles (j) around site i indicate lattice shells used for calculating local concentration at i .

concentrations.

The evolving alloy CP during the growth of QDs is simulated by minimizing the Gibbs free energy, $G = H - TS$. $H = \Omega x_A x_B = E_{el} + E_s$ is the enthalpy. E_{el} is the total elastic strain energy including the microscopic strain energy due to the bond distortion in the QDs and the macroscopic strain energy associated with the lattice mismatch between the QDs and the substrate. It is calculated using an atomistic strain model [10], based on harmonic potentials, that includes nearest-neighbor (NN), next-NN (NNN), and bond-bending (BB) interactions. E_s is the QD surface energy, i.e., the bond-breaking energy at the surface without consideration of surface reconstruction. Using the experimental elastic constants, our model produces the interaction parameters of mixing $\Omega_{\text{Ge}_x\text{Si}_{1-x}} = 1.83 \times 10^{-5}x + 0.02$, which agree well with previous first principles [11] results. $S = -k \sum_{\text{Lattice } i=1}^N S_i = -k \sum_{\text{Lattice } i=1}^N \left\{ \frac{1}{n} \sum_{\text{Shell } j=1}^n [x_{ij} \ln(x_{ij}) + (1 - x_{ij}) \ln(1 - x_{ij})] \right\}$ is the configuration entropy of mixing. It is calculated using a regular-solution-shell-model. The local alloy concentration at a given lattice site i , used to calculate S_i , is determined by averaging lattice shells (j) centered at i , as illustrated in Fig. 1, and tests have been done for the shell size and shell number to ensure convergence.

First, as a reference, we simulated the equilibrium CPs of strained alloy QDs with different shapes, as shown in Fig. 2. For a given QD shape, we simulated QDs with base size ranging from 10nm to 60nm , and the results are found to be qualitatively size independent as long as the size is large enough for the convergence of shell-model entropy calculations which is $\sim 30\text{nm}$. The results shown are with 60nm base size. To reach the equilibrium, all atoms in the QD are allowed to exchange positions and relax to minimize the total energy using an MC algorithm at a typical growth temperature of 900K . Different temperatures do not alter the qualitative composition patterns, but change slightly the quantitative composition profiles. For simplicity, interdiffusion at the

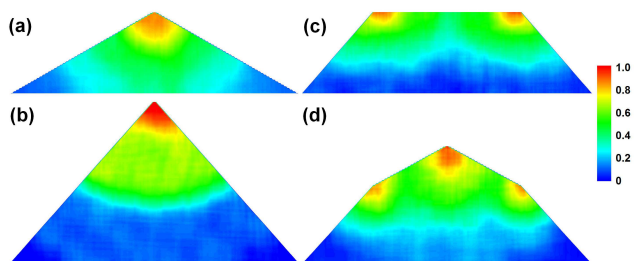


FIG. 2: (Color online) Equilibrium CPs of $\text{Ge}_{0.3}\text{Si}_{0.7}$ QDs with different contact angles and shapes: (a) shallow angle pyramid, (b) steep angle pyramid, (c) truncated pyramid, (d) dome. Ge concentrations are color-coded in a contour plot, as marked by color bars.

QD/substrate interface is excluded. Figures 2 (a) and (b) show the equilibrium CP of two pyramidal QDs with different contact angles. Figures 2 (c) and (d) show the results of a truncated-pyramid and a dome shaped QD, respectively. They agree well with previous finite element [5] and MC calculations [6]. The most prominent feature is the segregation of the strained element (Ge) to the top apex and upper corners of the QD, where the strain is most relaxed [1], and simultaneously the unstrained element (Si) to the corners of the base. The Ge concentration decreases continuously from the upper corners towards the base and base corners. These general features are qualitatively same for all QDs independent of their size and shape.

Next, we focus on the non-equilibrium QD CPs, controlled by kinetic factors, in particular the kinetic growth modes. Although the thermodynamic equilibrium CP may be reached in very small QDs grown at relatively high temperatures, where diffusion allows redistribution of the alloy components within the entire dot, it is generally not expected to occur. This is because bulk diffusion is negligible at typical growth temperatures due to the high energy barrier, for example 4-5 eV for Ge diffusion in Si [12]. However, the barriers are greatly reduced at surfaces. For example, surface diffusion barriers of 0.5-1.0 eV are reported for Si and Ge on Si(100) [13, 14]. The increased diffusion also occurs in the subsurface region [15]. This allows local equilibrium CPs to be established in the near-surface regions during growth, including the effect of Ge surface segregation [9]. Consequently, the kinetic growth mode, which dictates the surface mass transport and alloy mixing via surface diffusion at the growth front, becomes a key factor in determining the kinetically limited CP.

In order to reveal the underlying relationship between the non-equilibrium CPs of QDs and the growth mode, we investigated the effects of two typical kinetic modes: layer-by-layer growth (LG) versus faceted growth (FG). The reason we consider LG in addition to FG is because experiments [16] showed that SiGe islands first grow in a nonfaceted structure via the LG before transforming into the faceted pyramidal structure. Therefore, the alloy composition in the final faceted island is affected by the LG in the early stage of growth. Also, some observed composition profiles [3, 4] agree well with the simulation results from LG as shown below.

Figure 3(a) illustrates the typical Stranski-Krastonow (SK) epitaxial growth process of a strained QD. In the LG [Fig. 3(b)], QD growth proceeds in the substrate surface normal direction, with successive nucleation and growth of new surface layers on top of the previous surface layers. This results in a stepped-mound or wedding cake QD structure. In the FG [Fig. 3(c)], the QD growth proceeds in the facet normal direction, with successive nucleation and growth of new facets on top of the previous facets. This often forms a pyramidal structure [17].

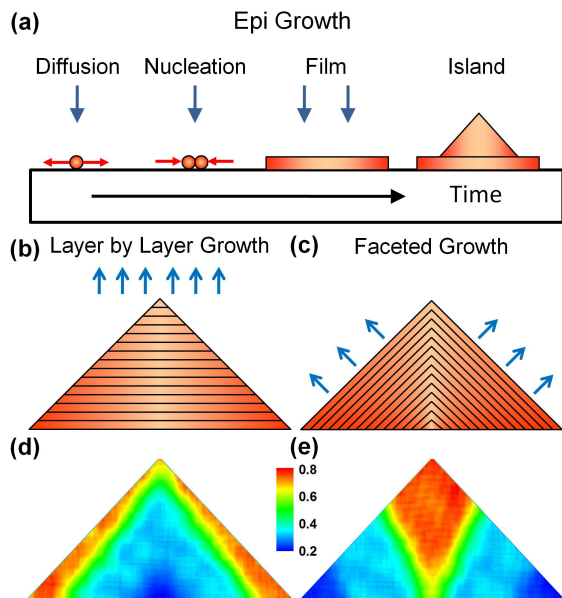


FIG. 3: (Color online) (a) Schematic of the typical SK epitaxial growth process of a strained QD. (b) Schematic illustration of the LG of a QD. (c) the FG of a QD. (d) Contour plot of the CP of a QD with a triangle-shaped Si-rich core, resulting from the LG. (e) Contour plot of the CP of a QD with a V-shaped Ge-rich core, resulting from the FG. The color bar marks the Ge concentration.

As the faceted QD grows larger, new facets may form transforming the QD into a dome shape [18]. Because qualitatively similar behavior is observed for different QD shapes, in what follows we show only the results for pyramidal QDs for both growth modes, to facilitate an easier comparison.

As a limiting case, we first assumed that in both growth modes, the local equilibrium CP is reached only in the outmost surface (or facet) layer and the equilibrated surface CP is subsequently frozen upon the growth of the subsequent layers. Such kinetically limited growth leads to the spontaneous formation of core-shell structured QDs [Figs. 3(d) and (e)]. The LG yields structures with cores rich in the unstrained component [Fig. 3(d), $x_{\text{Si}} > 0.8$ in the core], while the FG yields structures with cores rich in the strained component [Fig. 3(e), $x_{\text{Ge}} > 0.8$ in the core]. These growth-mode-limited non-equilibrium CPs are distinctively different from the equilibrium CPs shown in Fig. 2(b).

The above results can be qualitatively understood in terms of different strain relaxation mechanisms associated with the different growth modes. In the LG, the growth front is flat. When the atoms are equilibrated within this flat layer, strain relaxation results in a "lateral" phase separation with the strained component (Ge)

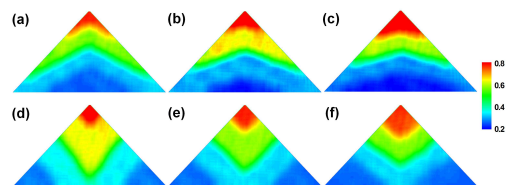


FIG. 4: (Color online) Non-equilibrium Ge CPs of heteroepitaxial $\text{Ge}_{0.3}\text{Si}_{0.7}$ QDs grown on Si substrates, when local equilibration is achieved for several surface layers at the growth front. The top panel shows the triangle-shaped Si-rich core resulting from the LG with mixing of (a) 4, (b) 7, and (c) 10 surface layers. The bottom panel shows the V-shaped Ge-rich core resulting from the FG with mixing of (d) 4, (e) 7, and (f) 10 facet layers. The color bar marks the Ge concentration.

segregating to the outside (the most relaxed region) and the unstrained component (Si) to the center of the surface layer. In contrast, in the FG, the growth front is inclined at a fixed contact angle with the substrate surface. When the atoms are equilibrated within this inclined facet layer, strain relaxation results in a "vertical" phase separation with Ge segregating to the top (the most relaxed region) and Si to the bottom of the facet. The segregated surface CPs are successively frozen in as the growth proceeds. Such lateral versus vertical segregation patterns leads to the different overall core-shell compositional structures in the LG versus FG.

A notable difference in the core-shell structures of QDs is seen, with either a triangle core shape in Fig. 3(d) or a V-shape in Fig. 3(e). This is because as the QD grows larger in the LG, the growth front becomes smaller, i.e., fewer atoms are contained within the surface layer. Consequently, fewer Ge atoms are segregated to the outside in subsequent layers, leading to the triangular core shape in Fig. 3(d). In contrast, as the QD grows larger in the FG, the growth front becomes larger, so that more Ge atoms are segregated to the top in the subsequent facets, leading to the V-shaped core in Fig. 3(e).

The constraint of equilibration only in the outmost surface (facet) layer is likely too severe, i.e., enhanced diffusion and hence local equilibration may extend to several subsurface layers, as suggested previously [15, 19]. Thus, we have studied the effects of varying the sub-surface diffusion depth on the CPs of QDs [20]. Figure 4 shows the calculated CPs of QDs grown by the LG [Figs. 4(a-c)] versus the FG [Figs. 4(d) and (e)] with the mixing depths of 4 [Figs. 4(a) and (d)], 7 [Figs. 4(b) and (e)] and 10 layers [Figs. 4(c) and (f)], respectively. These results clearly show the impact of diffusion depth on the CP. Increasing the atom mixing depth causes the core-shell structure to gradually disappear and the overall CPs obtained from both growth modes are seen to converge towards the equilibrium CP [Fig. 1(a)].

Next, we will examine some experimental QD CPs in light of our simulations. We did not find experimental CPs resemble the predicted triangle-shaped core in Fig. 3(d). This suggests that QDs either form via the FG or via the LG with multi-layer surface mixing. We tend to believe the multi-layer mixing is the reason, as the LG do occur. For example, recent work by Rastelli *et al.* [3] has shown lateral variations as well as vertical segregation gradients of Ge composition in strained GeSi QDs grown on Si(100) surface. Vertically, the Ge composition decreases from the top to the bottom in both small domes and large faceted pyramids. Laterally, however, the Ge composition is enhanced in the shell for domes but enhanced in the core for pyramids. Comparing these experimental CPs with our simulation results (Fig. 4), we can draw some interesting inference that the small GeSi QDs first grow via the LG, followed by a transition to the FG for larger QDs. These are consistent with suggestions made previously based on other evidences [16, 21]. On the other hand, the predicted V-shaped CP shown in Fig. 3(e) has been observed in $\text{In}_{0.5}\text{Ga}_{0.5}\text{As}$ QDs grown on GaAs substrate by Liu *et al.* [22], which exhibited truncated V-shaped In-rich cores after the QD apex was dissolved. This indicates that the InGaAs QDs were grown on GaAs substrate via the FG, having a consecutive "vertical" phase separation in the facets as the QD grows, consistent with the original analytical model explanation [22].

The above results also suggest that the SiGe QDs form without nucleation [16], first grow as stepped-mounds via LG and then transform into the faceted pyramid and grow via FG, while the InGaAs QDs form directly via nucleation of the faceted island and grow via FG. So, our study is able to correlate, for the first time, the different alloy compositions in SiGe vs. InGaAs islands with their different growth modes and processes.

In conclusion, using a newly developed atomistic-strain-model MC method, we have simulated the none-equilibrium CPs of epitaxial QDs. Our studies reveal a striking correlation between the CPs of QDs and their growth mode, i.e., LG versus FG, which provides a unique method to assess the QD growth modes and formation mechanism by comparing the simulations with the experiments. Conversely, it also suggests a possible method for controlling the CP of QDs by selecting the growth mode. In general, the growth mode is determined by growth parameters and/or by surface conditions. One effective way of affecting the growth mode is by the surfactant effects [23], which have been shown to alter the alloy CP [24, 25]. Thus, our findings form a fundamental basis for developing useful technologies to tailor and control the CPs of QDs, which can also be generally applicable to other self-assembled strained alloy nanostructures, such as nanowires.

This work was supported by the DOE-BES (Grant No. DE-FG02-04E46148) and the Cao Group. We thank the Center for High Performance Computing at University of Utah for providing the computing resources. We also thank Oliver Schmidt and Anil Virkar for helpful discussions.

*Email: fliu@eng.utah.edu

-
- [1] F. Liu and M. G. Lagally, *Surf. Sci.* **386**, 169 (1997).
 - [2] G. B. Stringfellow, *J. Cryst. Growth* **312**, 735 (2010).
 - [3] A. Rastelli *et al.*, *Nano Lett.* **8**, 1404 (2008).
 - [4] A. Malachias *et al.*, *Phys. Rev. Lett.* **91**, 176101 (2003).
 - [5] N. V. Medhekar, V. Hegadekatte and V. B. Shenoy, *Phys. Rev. Lett.* **100**, 106104 (2008).
 - [6] F. Uhlík, R. Gatti and F. Montalenti, *J. Phys.: Condens. Matter* **21**, 084217 (2009).
 - [7] G. B. Stringfellow, *Organometallic Vapor Phase Epitaxy: Theory and Practice* (Academic Press, Boston, 1999).
 - [8] J. M. Reich, X. B. Niu, Y. J. Lee, R. E. Caffisch and C. Ratsch, *Phys. Rev. B* **79**, 073405 (2009).
 - [9] See EPAPS Document of supplementary material for results of 3D model simulations and results showing surface segregation.
 - [10] A. C. Schindler *et al.*, *Phys. Rev. B* **67**, 075316 (2003).
 - [11] A. Qteish and R. Resta, *Phys. Rev. B* **37**, 1308 (1988).
 - [12] G. L. McVay and A. R. DuCharme, *Phys. Rev. B* **9**, 627 (1974).
 - [13] D. J. Shu, F. Liu and X. G. Gong, *Phys. Rev. B* **64**, 245410 (2001).
 - [14] L. Huang, F. Liu, G. H. Lu and X. G. Gong, *Phys. Rev. Lett.* **96**, 016103 (2006).
 - [15] B. P. Uberuaga, M. Leskova, A. P. Smith, H. Jónsson and M. Olmstead, *Phys. Rev. Lett.* **84**, 2441 (2000).
 - [16] P. Sutter and M. G. Lagally, *Phys. Rev. Lett.* **84**, 4637 (2000); R. M. Tromp, F. M. Ross and M. C. Reuter, *Phys. Rev. Lett.* **84**, 4641 (2000).
 - [17] Y. W. Mo, D. E. Savage, B. S. Swartzentruber and M. G. Lagally, *Phys. Rev. Lett.* **65**, 1020 (1990).
 - [18] G. Medeiros-Ribeiro *et al.*, *Science* **279**, 353 (1998).
 - [19] F. Liu and M. G. Lagally, *Phys. Rev. Lett.* **76**, 3156 (1996).
 - [20] In the real growth, the degree of diffusion and mixing may vary from the surface layer to subsurface layers. This effect is implicitly treated here by varying the number of mixing layers. A more rigorous treatment will not alter our qualitative results and conclusions.
 - [21] G. H. Lu and F. Liu, *Phys. Rev. Lett.* **94**, 176103 (2005); J. Tersoff *et al.*, *Phys. Rev. Lett.* **89**, 196104 (2002).
 - [22] N. Liu, J. Tersoff, O. Baklenov, A. L. Holmes, Jr. and C. K. Shih, *Phys. Rev. Lett.* **84**, 334 (2000).
 - [23] R. M. Tromp and M. C. Reuter, *Phys. Rev. Lett.* **68**, 954 (1992).
 - [24] E. Rudkevich *et al.*, *Phys. Rev. Lett.* **81**, 3467 (1998).
 - [25] J. Y. Zhu, F. Liu and G. B. Stringfellow *Phys. Rev. Lett.* **101**, 196103 (2008).